Feasibility of combined use of intravascular ultrasound radiofrequency data analysis and optical coherence tomography for detecting thin-cap fibroatheroma

Sawada, Takahiro ; Shite, Junya ; Garcia-Garcia, Hector M. ; Shinke, Toshiro ; Watanabe, Satoshi ; Otake, Hiromasa ; Matsumoto, Daisuke ;…

(Citation)
European Heart Journal,29(2):1136-1146

(Issue Date)
2008-04-07

(Resource Type)
journal article

(Version)
Version of Record

European Heart Journal (2008) **29**, 1136–1146
doi:10.1093/eurheartj/ehn132

Feasibility of combined use of intravascular ultrasound radiofrequency data analysis and optical coherence tomography for detecting thin-cap fibroatheroma

Takahiro Sawada[1], Junya Shite[1]*, Hector M. Garcia-Garcia[2], Toshiro Shinke[1], Satoshi Watanabe[1], Hiromasa Otake[1], Daisuke Matsumoto[1], Yusuke Tanino[1], Daisuke Ogasawara[1], Hiroyuki Kawamori[1], Hiroki Kato[1], Naoki Miyoshi[1], Mitsuhiro Yokoyama[1], Patrick W. Serruys[2], and Ken-ichi Hirata[1]

[1]Division of Cardiovascular Medicine, Department of Internal Medicine, Kobe University Graduate School of Medicine, 7-5-1 Kusunoki-cho, Chuo-ku, Kobe, Hyogo, 650-0017, Japan; and [2]Thoraxcenter, Erasmus MC, Rotterdam, The Netherlands

Received 5 October 2007; revised 25 February 2008; accepted 6 March 2008; online publish-ahead-of-print 7 April 2008

Aims To evaluate the feasibility of the combined use of virtual histology (VH)-intravascular ultrasound (IVUS) and optical coherence tomography (OCT) for detecting *in vivo* thin-cap fibroatheroma (TCFA).

Methods and results In 56 patients with angina, 126 plaques identified by IVUS findings were analysed using both VH-IVUS and OCT. IVUS-derived TCFA was defined as an abundant necrotic core (>10% of the cross-sectional area) in contact with the lumen (NCCL) and %plaque-volume >40%. OCT-derived TCFA was defined as a fibrous cap thickness of <65 μm overlying a low-intensity area with an unclear border. Plaque meeting both TCFA criteria was defined as definite-TCFA. Sixty-one plaques were diagnosed as IVUS-derived TCFA and 36 plaques as OCT-derived TCFA. Twenty-eight plaques were diagnosed as definite-TCFA; the remaining 33 IVUS-derived TCFA had a non-thin-cap and eight OCT-derived TCFA had a non-NCCL (in discord with NCCL visualized by VH-IVUS, mainly due to misreading caused by dense calcium). Based on IVUS findings, definite-TCFA showed a larger plaque and vessel volume, %plaque-volume, higher vessel remodelling index, and greater angle occupied by the NCCL in the lumen circumference than non-thin-cap IVUS-derived TCFA.

Conclusion Neither modality alone is sufficient for detecting TCFA. The combined use of OCT and VH-IVUS might be a feasible approach for evaluating TCFA.

Keywords Thin-cap fibroatheroma • VH-IVUS • OCT • Necrotic core • Vessel positive remodelling

Introduction

Acute coronary syndrome (ACS) commonly results from plaque rupture,[1–3] and occasionally results from erosion or calcified nodules.[4,5] The pathologic features of plaque prone to rupture are a positively remodelled vessel, including a large necrotic core, a thin fibrous cap (<65 μm), and macrophage infiltration into the cap.[2,3] This entity is usually known as thin-cap fibroatheroma (TCFA).

The accurate detection of TCFA is vital for the diagnosis of vulnerable patients. New imaging modalities, such as virtual histology (VH)-intravascular ultrasound (IVUS) and optical coherence

* Corresponding author. Tel: +81 78 382 5846, Fax: +81 78 382 5859, Email: shite@med.kobe-u.ac.jp

tomography (OCT), were developed to precisely evaluate coronary plaques. Radiofrequency data analysis by VH-IVUS allows for atherosclerotic plaques to be classified as one of the four different types (fibrous, fibro-fatty, dense calcium, and necrotic core), and is especially useful for quantifying the necrotic core.[6,7] VH-IVUS cannot visualize the thin fibrous cap, however, because of its limited resolution (>100 μm). OCT, on the other hand, can provide a high resolution image (10–20 μm), but its penetration is limited (<2 mm).[8–11] OCT can visualize the thin fibrous cap, but is not able to detect a large and deep lipid core. Thus, it is difficult to diagnose TCFA using each modality alone. The combined use of these complementary imaging modalities, VH-IVUS and OCT, might result in more effective detection of TCFA.

The aim of this study was to elucidate the feasibility of the combined use of VH-IVUS and OCT to detect *in vivo* TCFA and to clarify the lesion characteristics of TCFA.

Methods

Patient and lesion population

Between August 2005 and March 2007, 402 patients with *de novo* ischaemic heart disease underwent coronary angiography in our hospital. Angina pectoris was identified as a significant coronary stenosis causing apparent myocardial ischaemia based on symptoms or electrocardiographic ST-T changes during an angina attack. To ensure safety during the OCT procedure, 121 patients were excluded because they had ST-segment elevation indicating an acute myocardial infarction or unstable angina pectoris warranting emergency percutaneous coronary intervention (PCI). Another 160 patients were excluded because 39 patients had chronic total occlusion, 20 patients had heavily calcified lesions that required rota-ablation, five patients had significant left main disease, and 96 patients had tortuous lesions expected to cause difficulty in advancing the IVUS and OCT catheters. Furthermore, we excluded six patients because they had vessels with a diameter >4.0 mm by angiography, which was too large to occlude blood flow. In the remaining 115 patients, 59 did not consent to the invasive intra-coronary examination, and the remaining 56 allowed us to perform the VH-IVUS and OCT examination. We identified plaques based on the IVUS findings and analysed each plaque using both VH-IVUS and OCT.

We assessed patient characteristics, including age, sex, body mass index, presence of coronary risk factors (hypertension, hyperlipidaemia, diabetes mellitus, smoking), and medication. Hypertension was defined as systolic blood pressure ≥140 mmHg, diastolic blood pressure ≥90 mmHg, or use of anti-hypertensive drugs. Hyperlipidaemia was defined as a present or past history of low-density lipoprotein–cholesterol level ≥140 mg/dl, or use of statin. Diabetes mellitus was defined as a fasting blood sugar >126 mg/dl and haemoglobin A1c ≥6.4%, or use of anti-diabetic medications (insulin or oral hypoglycaemics).

Binary examinations were performed if the patient experienced a severe angina attack or consented to a 6 month follow-up study (21 patients). This study was approved by the Ethics Committee of Kobe University.

Quantitative coronary arteriography measurement

Coronary angiogram was performed after intracoronary injection of nitroglycerin (250 μg), and the severity of stenosis was measured with a quantitative coronary arteriography cardiovascular measurement system (CMS-Medis Medical Imaging Systems, Leiden). We assessed traditional lesion types using the American Heart Association/American College of Cardiology's classification, and mapped the plaque location (proximal, mid, or distal vessel) angiographically. Because some plaques were completely undetectable by angiography, information from the IVUS was used to determine the plaque location.

Intravascular ultrasound procedure and quantitative coronary ultrasound measurement

A 2.9Fr 20 MHz IVUS catheter (Eagle-Eye™; Volcano Therapeutics, Inc., Rancho Cordova, CA, USA) was inserted into the coronary artery more than two-thirds distal, and subsequently pulled back with the aid of motorized pullback system (0.5 mm/s). The IVUS images obtained were digitized for quantitative and qualitative analysis according to the criteria of the American College of Cardiology's Clinical Expert Consensus Document on IVUS.[12] A 3D reconstruction of volumetric gray-scale IVUS data was performed using a semi-automated quantitative coronary ultrasound cardiovascular measurement system (CMS-Medis Medical Imaging Systems). If the patient required PCI, we obtained the IVUS data before the PCI procedure. Plaques in the same artery were considered to be separate lesions if the reference segment between them was >5 mm; otherwise, they were considered to be part of a single lesion.

IVUS data recorded on CD-ROM for off-line analysis were used to calculate the lesion length, lumen volume, vessel volume, and plaque volume (vessel volume–lumen volume) based on manual counter-detection of both the lumen and vessel interfaces in each cross-sectional frame. We then used these data to calculate %plaque-volume (plaque volume/vessel volume × 100) and remodelling index (vessel cross-sectional area of minimum lumen site/averaged reference vessel cross-sectional area).

Virtual histology analysis and definition of intravascular ultrasound-derived thin-cap fibroatheroma

Raw radiofrequency data of these lesions were stored on a DVD for off-line quantitative analysis, and plaques were classified by version 2.0 VH software into fibrotic, fibro-fatty, dense calcium, and necrotic core components. Plaque components were represented as a ratio of plaque volume (%fibrous, %fibro-fatty, %dense-calcium, %necrotic-core). Using a previously reported definition,[13] we defined IVUS-derived TCFA as a lesion meeting the following two criteria in at least three consecutive frames: (1) focal necrotic core-rich lesions (%necrotic-core >10%) without evident overlying fibrous tissue and (2) %plaque-volume ≥40%.

An independent investigator at the Erasmus Medical Center quantified the area of the necrotic core in contact with the lumen (NCCL) as well as the major confluent NCCL area and angle occupied by the NCCL in the lumen circumference using a program implemented in MATLAB™ (MathWorks, Natick, MA, USA). The angle formed by the connected necrotic core pixels on the border of the lumen was measured with respect to the lumen centre of gravity (*Figure 1*).[14]

Optical coherence tomography examination and definition of optical coherence tomography-derived thin-cap fibroatheroma

After the IVUS procedure, OCT examination was performed as previously described.[8] Briefly, an over-the-wire type occlusion balloon

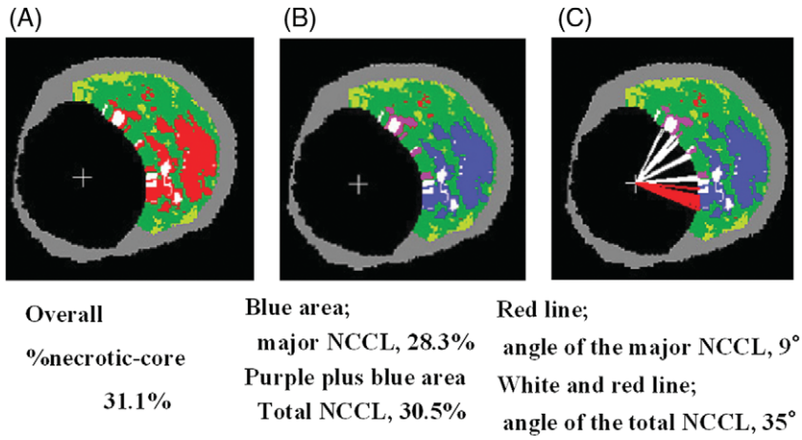

Figure 1 An example of selective quantification of the necrotic core in contact with the lumen (NCCL). (*A*) The original virtual histology-intravascular ultrasound cross-sectional area. (*B*) The blue area was selectively quantified as the major confluent NCCL areas and blue plus purple areas indicate total NCCL areas. (*C*) Measurement of the angle occupied by the total NCCL (white and red line) and the angle occupied by the major confluent NCCL (red line).

Table 1 Clinical characteristics

	Patients without definite-TCFA	Patients with definite-TCFA	*P*-value
Number (*n*)	32	24	
Age (year)	68.1 ± 8.7	70.1 ± 8.2	NS
Male (*n*)	18	17	NS
Body mass index (kg/m^2)	23.7 ± 2.8	24.6 ± 2.8	NS
Risk factor (*n*)			
Hypertension	25	19	NS
Hyperlipidemia	24	17	NS
Diabetes mellitus	18	11	NS
Smoke	10	9	NS
Acute coronary syndrome (*n*)	2	3	NS
Diseased vessel (1/2/3)	9/19/4	10/9/5	NS
Statin (*n*)	21	16	0.07
(Month)	15.0 (6.8, 34.5)	9.0 (6.3, 17.0)	0.09
ARB/ACEI (*n*)	21	19	NS
(Month)	22.0 (15.0, 96.0)	15.0 (12.0, 22.5)	NS
Total cholesterol (mg/dL)	177.1 ± 23.9	193.1 ± 40.2	0.07
LDL−cholesterol (mg/dL)	99.3 ± 17.4	112.8 ± 35.1	NS
HDL−cholesterol (mg/dL)	54.2 ± 21.6	52.1 ± 12.8	NS
Triglyceride (mg/dL)	132.6 ± 100.0	154.0 ± 93.0	NS
Fasting blood sugar (mg/dL)	115.1 ± 36.0	118.4 ± 40.2	NS
HemoglobinA1c (%)	6.2 ± 1.2	5.9 ± 0.9	NS
hs-CRP (mg/dl)	0.12 ± 0.11	0.15 ± 0.20	NS

Data are expressed mean value ± SD or median (25th, 75th percentile). $P < 0.05$ was considered statistically significant.
ARB, angiotensin receptor blocker; ACEI, angiotensin converting enzyme inhibitor; hs-CRP, high-sensitive C-reactive protein.

catheter (Helios™, LightLab Imaging Inc., Westford, MA USA) and an OCT imaging, probe (ImageWire™, LightLab Imaging Inc.) were inserted into the coronary artery more than two-thirds distal. The entire vessel length was imaged with an automatic pullback device at 1 mm/s, and OCT data were recorded on a CD-ROM for off-line analysis.

An OCT image of a signal-poor lesion with an unclear border was diagnosed as a lipid core and a signal-rich homogenous lesion overlying lipid content was diagnosed as a fibrous cap.[9–11] The thinnest part of the fibrous cap was measured three times and the average value calculated. Because the previous histopathology report revealed that 95% of the fibrous cap thickness near a rupture site was <65 μm,[15] a lesion whose fibrous cap thickness at the thinnest part was <65 μm was diagnosed as OCT-derived TCFA.

Comparison of virtual histology-intravascular ultrasound and optical coherence tomography images and definition of definite-thin-cap fibroatheroma

We compared the VH-IVUS and OCT images of identical lesions using the locations of side branches, longitudinal plaque distribution, or calcification as landmarks. If the plaque met the criteria of both the IVUS-derived TCFA and OCT-derived TCFA, we diagnosed it as definite-TCFA. If IVUS-derived TCFA did not have a thin fibrous cap (<65 μm) by OCT measurement, we diagnosed it as non-thin-cap IVUS-derived TCFA. If VH-IVUS did not detect an NCCL that was detected by OCT-derived TCFA, the plaque was diagnosed as non-NCCL OCT-derived TCFA.

To assess intra- and inter-observer variability, all VH-IVUS and OCT data were read by two independent observers. The first observer repeated a blind analysis of all the data at two separate time points (with at least 1 month interval between the two analyses). If there was discordance of either the IVUS- or OCT-derived TCFA diagnosis between the two observers, a consensus diagnosis was obtained with repeated off-line readings.

Statistical analysis

This is a pilot study that compared the data between VH-IVUS and OCT. Because a previous study demonstrated that plaque volume, vessel remodelling, necrotic core volume, and circumference were associated with an unstable plaque type,[2,16] we hypothesized that the factors indicative of thin fibrous cap in IVUS-derived TCFA were %plaque-volume, remodelling index, and angle occupied by NCCL in the lumen circumference. Thus, the sample size was based on the preliminary data obtained in our laboratory and was determined on the basis of the following assumptions: A type-I error of 0.05 (two-sided); power of 80%; difference in the %plaque-volume, remodelling index, and the NCCL angle between definite TCFA and non-thin-cap IVUS-derived TCFA of 8.0%, 0.1, and 30°, respectively, and a standard deviation of 8.0, 0.12, and 35, respectively. Therefore, the minimum required sample size was 23 lesions in each group. We stopped recruitment at 20 months, because the power of these data was beyond 99.9%. Because of the limited sample size of non-NCCL OCT-derived TCFA (eight lesions), the data for this group were considered exploratory.

Statview version 5.0 (SAS, Cary, NC, USA) was used for the data analysis. Qualitative data are presented with frequencies and quantitative data are shown as medians (25th and 75th percentiles) or mean ± SD when indicated. Comparison of laboratory data between the two groups was performed using the unpaired *t*-test. If the data were not normally distributed, as determined by Kolmogorov–Smirnov analysis, the data were analysed using a Mann–Whitney test. A two-sided *P*-value of <0.05 was considered statistically significant.

Angiographical data, gray-scale IVUS and VH-IVUS data were analysed using random-effects generalized least-squares regression in order to account for repeated measurements on individual patients. Wald's test was used for assessing differences in means between plaque type categories. Fitted models were used in calculating predicted means and their 95% confidence intervals (CIs). For the values in *Table 2*, a model with two categories of plaque types (definite-TCFA and non-TCFA) was fit. For the values displayed in *Tables 3* and *4*, a separate model with four categories of plaque types (definite-TCFA and the three subcategories of non-TCFA plaque types) was fit. Predicted means and CIs for definite-TCFA in *Tables 3* and *4* occasionally differ slightly from those in *Table 2*, because separate models were used. An adjusted *P*-value of <0.0167 (0.05/3, Bonferroni's correction for multiple comparisons) was used as the threshold for significance to avoid an inflated type-I error because three pairwise planned comparisons were made.

To assess the inter- and intra-observer variability, the results were compared using the κ-test of concordance for the categorical data and Bland–Altman plot was fulfilled for continuous variables.

Results

Feasibility of virtual histology-intravascular ultrasound and optical coherence tomography examinations

In 56 patients, 82 diseased vessels were observed with VH-IVUS and OCT without any complications. We identified 126 plaques in the 82 diseased vessels. The average procedure time of VH-IVUS and OCT, including preparation of both devices, was 18.7 ± 4.4 min. The mean evaluation length by VH-IVUS was 48.6 ± 16.3 mm and that measured by OCT was 44.5 ± 12.8 mm. The average balloon occlusion time for one-time OCT imaging was 49.8 ± 11.4 s.

Identification of intravascular ultrasound-, optical coherence tomography-derived thin-cap fibroatheroma, and definite-thin-cap fibroatheroma

Of 126 plaques, VH-IVUS observations identified 61 plaques (48.4%) as IVUS-derived TCFA, and OCT examination diagnosed 36 plaques (28.6%) as OCT-derived TCFA. Twenty-eight (22.2%) of the plaques met both criteria for TCFA and were diagnosed as definite-TCFA. The remaining 33 IVUS-derived TCFA (26.2%) were diagnosed as non-thin-cap IVUS-derived TCFA (mean fibrous cap thickness by OCT was 99.0 ± 13.3 μm) and the remaining eight OCT-derived TCFA (6.3%) were diagnosed as non-NCCL OCT-derived TCFA. The positive ratio of VH-IVUS for detecting definite TCFA was 45.9% and that of OCT was 77.8%. A summary of the lesion diagnoses is shown in *Figure 2* and representative cases of non-thin-cap IVUS-derived TCFA,

Table 2 Comparison of angiographical data, gray-scale intravascular ultrasound, and virtual histology-intravascular ultrasound data between non-thin-cap fibroatheroma and definite-thin-cap fibroatheroma

	Non-TCFA (n = 98)	Definite-TCFA (n = 28)	P-value (vs. definite-TCFA)
Left anterior descending artery	40	12	
Left circumflex artery	16	4	
Right coronary artery	42	12	NS
Type of lesion			
A/B1	84	22	
B2/C	14	6	NS
Location of lesion			
Proximal	21	15	
Mid	56	12	
Distal	21	1	0.002
Quantitative coronary arteriography data			
Reference vessel diameter (mm)	2.42 (2.30, 2.55)	2.53 (2.30, 2.76)	NS
Minimum lumen diameter (mm)	1.84 (1.62, 2.05)	1.84 (1.62, 2.05)	NS
%Area-stenosis (%)	34.3 (30.6, 38.0)	45.1 (38.2, 52.1)	0.007
Gray-scale IVUS measurements			
Plaque volume (mm^3/cm)	71.2 (53.2, 89.3)	96.1 (73.7, 118.4)	0.0001
Vessel volume (mm^3/cm)	139.9 (109.0, 176.5)	162.1 (124.7, 200.0)	0.004
Plaque length (mm)	12.8 (11.1, 14.6)	17.5 (14.4, 20.6)	NS
%Plaque-volume (%)	48.6 (46.8, 50.4)	56.5 (53.3, 59.7)	$<$0.0001
Remodelling-index	1.06 (1.03, 1.08)	1.21 (1.17, 1.25)	$<$0.0001
VH measurements			
%Fibrous	62.1 (60.3, 65.1)	56.8 (52.6, 61.0)	0.01
%Fibro-fatty	13.4 (11.8, 14.9)	13.5 (10.7, 16.4)	NS
%Dense-calcium	8.8 (7.3, 10.4)	9.9 (7.0, 10.4)	NS
%Necrotic-core	15.3 (13.7, 16.9)	20.0 (17.0, 23.0)	0.006

Data are expressed predicted means and their 95% CIs. For the values in this table, a model with two categories of plaque types (definite-TCFA and non-TCFA) was fit. An adjusted P-value of < 0.0167 (Bonferroni's correction for multiple comparisons) was considered significant.

non-NCCL OCT-derived TCFA, and definite-TCFA are shown in *Figure 3A–C*, respectively.

Baseline characteristics and laboratory data

At least one definite-TCFA was identified in 24 patients (42.9%) but not in the other 32 patients (57.1%). The baseline characteristics and laboratory data for these two patient groups were summarized in *Table 1*. There were no differences in age, sex, body mass index, or cardiac risk factors between the two groups. In the present study, five (8.9%) patients had ACS that did not warrant emergency PCI and most of our study population (91.1%) had stable angina. Among the five ACS patients, three had at least one definite-TCFA.

Although patients without definite-TCFA tended to take statins for a longer duration and their total cholesterol level tended to be lower than that in patients with definite-TCFA ($P = 0.07$, both), there were no significant differences in the lipid profiles, blood sugar profiles, and high-sensitive C-reactive-protein between the two groups.

Comparison of non-thin-cap fibroatheroma and definite-thin-cap fibroatheroma

The summarized angiographical data, gray-scale IVUS, and VH-IVUS data for non-TCFA and definite-TCFA are shown in *Table 2*. There were no differences in lesion type, reference diameter, and minimum lumen diameter between the two groups, but definite-TCFA showed significantly higher %area-stenosis and tended to be located in the proximal part of the vessel ($P = 0.007$ and $P = 0.002$, respectively). Based on the gray-scale IVUS analysis, plaque volume and vessel volume of definite-TCFA were significantly higher than those of non-TCFA ($P = 0.0001$ and $P = 0.004$, respectively). Also, the values for %plaque-volume and the vessel remodelling index of definite-TCFA were significantly higher than those of non-TCFA ($P < 0.0001$, both). VH analysis showed that the %necrotic-core of definite-TCFA was significantly higher than that of non-TCFA and %fibrous of definite-TCFA was significantly lower than that of non-TCFA ($P = 0.006$ and $P = 0.01$, respectively).

Table 3 Comparison of angiographical data, gray-scale intravascular ultrasound, and virtual histology-intravascular ultrasound data between non-thin-cap intravascular ultrasound-derived thin-cap fibroatheroma and definite-thin-cap fibroatheroma

	Non-thin-cap IVUS-derived TCFA (n = 33)	Definite-TCFA (n = 28)	P-value (vs. definite-TCFA)
Quantitative coronary arteriography data			
Reference vessel diameter (mm)	2.40 (2.19, 2.61)	2.52 (2.31, 2.74)	NS
Minimum lumen diameter (mm)	1.92 (1.71, 2.12)	1.84 (1.62, 2.05)	NS
%Area-stenosis (%)	35.4 (28.6, 48.1)	45.1 (38.2, 52.1)	NS
Gray-scale IVUS measurements			
Plaque volume (mm^3/cm)	65.3 (39.3, 91.4)	96.3 (75.6, 117.0)	0.001
Vessel volume (mm^3/cm)	132.6 (89.1, 176.2)	162.0 (127.4, 196.4)	0.01
Plaque length (mm)	13.4 (10.5, 16.4)	17.4 (14.4, 20.5)	NS
%Plaque-volume (%)	48.1 (45.0, 51.1)	56.5 (53.4, 59.7)	0.0001
Remodelling index	1.10 (1.06, 1.13)	1.21 (1.17, 1.25)	0.0005
VH measurements			
%Fibrous	58.9 (55.1, 62.7)	57.0 (53.1, 60.9)	NS
%Fibro-fatty	12.3 (9.5, 15.1)	13.5 (10.7, 16.4)	NS
%Dense-calcium	10.5 (7.9, 13.1)	9.9 (7.3, 12.6)	NS
%Necrotic-core	18.6 (15.7, 21.4)	20.0 (17.0, 22.9)	NS
Major NCCL area (mm^2)	0.62 (0.46, 0.94)	1.15 (0.77, 1.39)	0.003
Total NCCL angle (degree)	54.6 (35.6, 73.5)	89.4 (63.6, 112.4)	0.0003
Major NCCL angle (degree)	19.0 (15.1, 21.2)	29.0 (20.2, 28.1)	0.005

Data are expressed predicted means and their 95% CIs. For the values in this table, a model with four categories of plaque types (definite-TCFA and three subcategories of non-TCFA plaque types) was fit. An adjusted P-value of <0.0167 (Bonferroni's correction for multiple comparisons) was considered significant.
NCCL, necrotic core contact with lumen.

Table 4 Comparison of angiographical data, gray-scale intravascular ultrasound, and virtual histology-intravascular ultrasound data between non-necrotic core in contact with the lumen optical coherence tomography-derived thin-cap fibroatheroma and definite-thin-cap fibroatheroma

	Non-NCCL OCT-derived TCFA (n = 8)	Definite-TCFA (n = 28)	P-value (vs. definite-TCFA)
Quantitative coronary arteriography data			
Reference vessel diameter (mm)	3.26 (2.85, 3.60)	2.52 (2.31, 2.74)	0.002
Minimum lumen diameter (mm)	2.50 (2.10, 2.90)	1.84 (1.62, 2.05)	0.004
%Area-stenosis (%)	38.8 (25.7, 47.8)	45.1 (38.2, 52.1)	NS
Gray-scale IVUS measurements			
Plaque volume (mm^3/cm)	122.5 (87.8, 157.2)	96.3 (75.6, 117.0)	NS
Vessel volume (mm^3/cm)	232.5 (171.9, 285.7)	162.0 (127.4, 196.4)	0.01
Plaque length (mm)	19.3 (13.6, 24.9.4)	17.4 (14.4, 20.5)	NS
%Plaque-volume (%)	52.9 (47.0, 58.8)	56.5 (53.4, 59.7)	NS
Remodelling index	1.04 (0.97, 1.12)	1.21 (1.17, 1.25)	0.003
VH measurements			
%Fibrous	49.8 (42.6, 56.9)	57.0 (53.1, 60.9)	NS
%Fibro-fatty	12.8 (7.4, 18.1)	13.5 (10.7, 16.4)	NS
%Dense-calcium	19.3 (14.3, 24.3)	9.9 (7.3, 12.6)	0.01
%Necrotic-core	17.3 (11.8, 22.7)	20.0 (17.0, 22.9)	NS

Data are expressed predicted means and their 95%*CIs*. For the values in this table, a model with four categories of plaque types (definite-TCFA and three subcategories of non-TCFA plaque types) was fit. An adjusted P-value of <0.0167 (Bonferroni's correction for multiple comparisons) was considered significant.

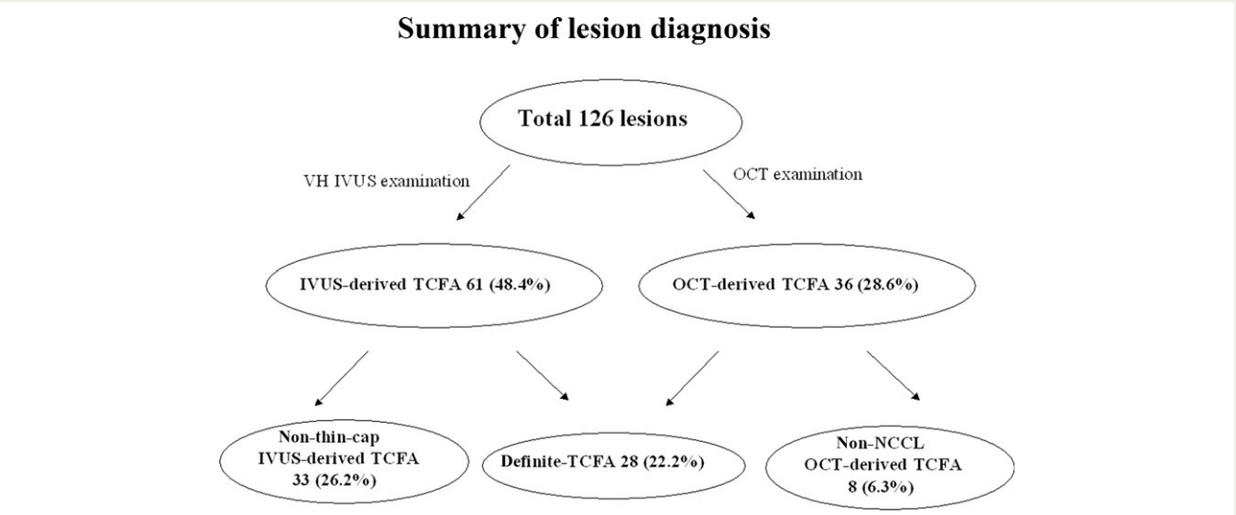

Figure 2 Among 126 lesions in 56 cases, virtual histology-intravascular ultrasound (VH-IVUS) diagnosed 61 lesions (48.4%) as IVUS-derived thin-cap-fiberatheroma (TCFA) and optical coherence tomography (OCT) revealed 36 lesions (28.6%) as OCT-derived TCFA. Twenty-eight lesions (22.2%) met the criteria of both IVUS-derived TCFA and OCT-derived TCFA and were diagnosed as definite-TCFA; 33 lesions were diagnosed as non-thin-cap IVUS-derived TCFA and eight lesions as non-NCCL OCT-derived TCFA.

Comparison of non-thin-cap intravascular ultrasound-derived thin-cap fibroatheroma and definite-thin-cap fibroatheroma

The summarized angiographical data, gray-scale IVUS, and VH-IVUS data for non-thin-cap IVUS-derived TCFA and definite TCFA are shown in *Table 3*. There were no differences in angiographical data between the two groups. Definite-TCFA, however, had a significantly larger plaque volume, vessel volume, %plaque-volume, and vessel remodelling index than non-thin-cap IVUS-derived TCFA ($P = 0.001$, $P = 0.01$, $P = 0.0001$ and $P = 0.0005$, respectively). Although there were no significant differences in the ratio of plaque components in the VH-IVUS analysis, definite-TCFA had a significantly larger major confluent NCCL area and a larger total angle occupied by NCCL in the lumen circumference compared with non-thin-cap IVUS-derived TCFA ($P = 0.003$ and $P = 0.0003$, respectively).

Comparison of non-necrotic core in contact with the lumen optical coherence tomography-derived thin-cap fibroatheroma and definite-thin-cap fibroatheroma

The summarized angiographical data, gray-scale IVUS, and VH-IVUS data for non-NCCL OCT-derived TCFA and definite TCFA are shown in *Table 4*. The sample size of non-NCCL OCT-derived TCFA was small, thus we considered these data exploratory, but non-NCCL OCT-derived TCFA had a significantly larger %dense-calcium and vessel volume, and smaller vessel remodelling index than definite-TCFA ($P = 0.01$, $P = 0.01$ and $P = 0.003$, respectively). Furthermore, non-NCCL OCT-derived TCFA had a larger reference diameter and minimum lumen diameter than definite-TCFA ($P = 0.002$ and $P = 0.004$, respectively).

Intra- and inter-observer variability

The estimated limit of agreement for the intra- and inter-observer variability in the VH-IVUS and OCT measurements was reasonable based on the Bland–Altman plot (%necrotic–core by VH-IVUS; intra-observer; mean difference: 0.03%, upper two-standard deviation (2SD): 1.63% and lower 2SD: −1.68%, inter-observer; mean difference: 0.10%, upper 2SD; 2.00% and lower 2SD: −1.90%, fibrous cap thickness by OCT; intra-observer; mean difference: 0.6 μm, upper 2SD: 12.2 μm and lower 2SD: −13.4 μm, inter-observer; mean difference: 1.9 μm, upper 2SD: 13.8 μm and lower 2SD: −17.7 μm).

There was little intra- or inter-observer disagreement in the diagnosis of IVUS-derived TCFA (intra-observer; $\kappa = 0.87$, 95% CI, 0.79–0.96, inter-observer; $\kappa = 0.81$, 95% CI 0.71–0.91) and in the diagnosis of OCT-derived TCFA (intra-observer; $\kappa = 0.87$ 0.77–0.96, inter-observer; $\kappa = 0.77$, 0.65–0.90).

Patient follow-up

In 21 patients with binary angiography (11 patients with definite-TCFA and 10 patients without definite-TCFA; 13 lesions were definite-TCFA and 32 lesions were non-TCFA; average span 205.0 ± 68.0 days), four lesions required PCI because of increasing plaque size and a constricting lumen, and three of these were definite-TCFA. A representative case of definite-TCFA progression is shown in *Figure 4*.

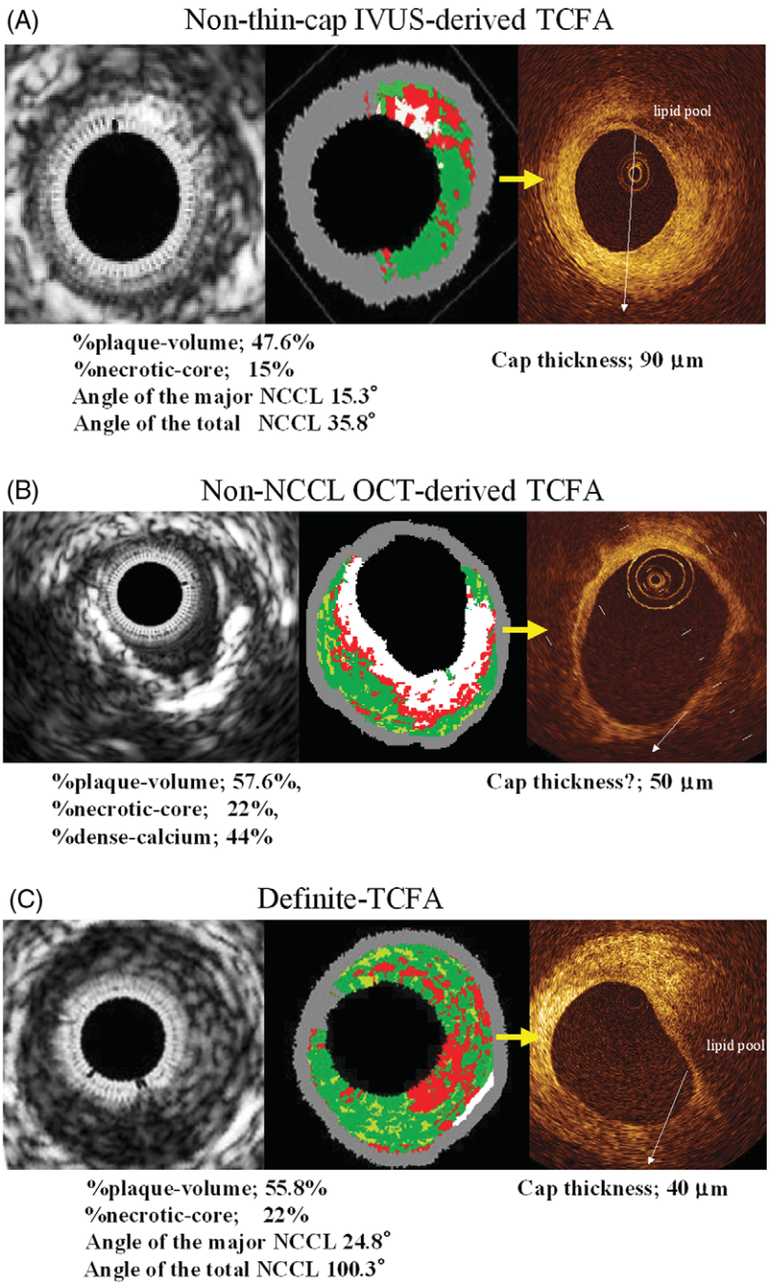

Figure 3 (*A*) A representative case of non-thin-cap IVUS-derived thin-cap fibroatheroma (TCFA). Virtual histology-IVUS shows 47.6% of %plaque-volume, 15% of %necrotic-core. The angle of the major NCCL was 15.3°, and that of the total NCCL was 35.8°. OCT shows signal-poor lesions with an overlying signal-rich band in the upper right quadrant. A signal-poor lesion indicates a lipid pool and signal-rich band indicates a fibrous cap. The fibrous cap thickness was 90 μm. (*B*) A representative case of non-NCCL OCT-derived TCFA. OCT identified a fibrous cap thickness of 50 μm which covers the low intensity area, but VH-IVUS did not identify the NCCL. (*C*) A representative case of definite-TCFA. Virtual histology-IVUS shows %plaque-volume of 55.8% and %necrotic-core of 22%. The angle of the major NCCL was 24.8°, and that of the total NCCL was 100.3°. Its minimum fibrous cap thickness was 40 μm.

Discussion

Pathology studies have demonstrated that acute coronary events most commonly arise from the disruption of TCFA. Several imaging modalities, including IVUS,[17] VH-IVUS,[13,14] angioscopy,[18] elastography,[19] and thermography,[20] have been used to detect TCFA. The sensitivity or specificity of these modalities for the detection of TCFA *in vivo*, however, has not been satisfactory.

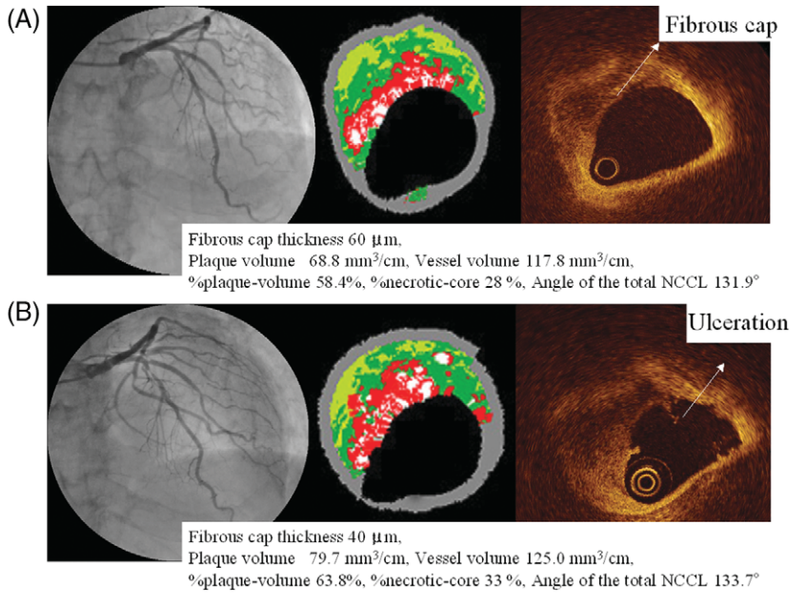

Figure 4 (*A*) Coronary angiography (CAG) revealed 50% stenosis in the mid-left anterior descending artery in July 2006. VH-IVUS revealed a 68.8 mm^3/cm plaque volume, 117.8 mm^3/cm vessel volume, 58.4% %plaque-volume, and 28% %necrotic-core. The fibrous cap thickness of this lesion was 60 μm by OCT measurement and this lesion was diagnosed as definite-TCFA. (*B*) After 6 months, because the patient experienced chest pain at rest with increased frequency, we performed CAG. The CAG revealed 90% stenosis at the site of the previous definite-TCFA lesion. VH-IVUS revealed an increase in plaque volume (68.8→79.7 mm^3/cm), vessel volume (117.8→125.0 mm^3/cm), %plaque-volume (58.4%→63.8%), and %necrotic-core (28%→33%). OCT revealed ulceration of the fibrous cap.

VH-IVUS for spectral analysis of radio-frequency data has the potential to detect TCFA. VH-IVUS is highly accurate for identifying plaque components both *in vitro* and *in vivo*.[6,7] Rodriguez-Granillo *et al.*[13] were the first to focus on the distribution of plaque components using VH-IVUS studies. They defined IVUS-derived TCFA based on pathologic data and demonstrated that the mean plaque volume and mean %necrotic-core of IVUS-derived TCFA were similar to previously reported histopathologic TCFA data. Thus, the ability of VH-IVUS to produce real-time assessment of plaque morphology has been established and might be useful for identifying TCFA. Because the maximum resolution of VH-IVUS is 100 μm, however, it is difficult to assess the thin fibrous cap (<65 μm).

Optical coherence tomography is a new imaging modality for detecting vulnerable plaque. OCT provides a high-resolution image and is able to evaluate detailed plaque morphology *in vivo*.[8–11] OCT, therefore, seems to have the potential to visualize the thin fibrous cap and detailed structures. The penetration of OCT is limited (<2 mm), so that it is frequently difficult to delineate large lipid plaques. Manfrini *et al.*[21] reported that OCT could be unreliable to differentiate areas with heterogenous composition because of its low signal penetration. In our study, eight OCT-derived TCFA lesions were not identified as an NCCL by VH-IVUS analysis. This discrepancy might be because of the penetration limitation of OCT. These lesions had a larger reference diameter, minimum lumen diameter, and minimum vessel volume than definite-TCFA ($P = 0.002$, $P = 0.004$, $P = 0.01$, respectively), and had severely calcified components compared with definite-TCFA ($P = 0.01$). When a target vessel or plaque is large, the optical signal might be attenuated by the plaque and failed to identify plaque morphology. It might also be sometimes difficult to discriminate between lipid and calcified lesions because both these appear as low-intensity images, usually differentiated in OCT by an unclear border (lipid) or a clear border (calcium). In this regard, large calcified lesions are likely to be misdiagnosed as TCFA by OCT examination. Therefore, it is difficult to detect TCFA using only one modality. Using a combination of complementary tools such as VH-IVUS and OCT might be a feasible approach for more accurate detection of TCFA.

Although the positive ratio of VH-IVUS for detecting definite-TCFA was 45.9% and that for OCT was higher than VH-IVUS (77.8%), OCT has several procedural limitations and is only used in selected hospitals. IVUS is now routinely used for PCI procedures. Thus, it is important to determine the criteria for TCFA by VH-IVUS. Previous IVUS and pathological studies showed that positive vessel remodelling is associated with an unstable clinical presentation and characteristic pathologic lesion types.[16,22,23] Kolodgie *et al.*[2] reported that whether the necrotic core is circumferential might be critical for determining the instability of a plaque, and they demonstrated that proximal coronary lesions with greater than 50% diameter stenosis with an necrotic core circumference >120° strongly suggests the presence of

plaque with a vulnerable morphology. In the present study, definite-TCFA identified by both modalities tended to locate in the proximal part of the vessels, areas with a higher %area-stenosis, %plaque-volume and more positively remodelled lesions in comparison to non-TCFA. These data are compatible with previously reported histopathologic data.[2,23] Furthermore, the major confluent NCCL area of definite-TCFA was larger and its NCCL occupied a larger circumference of the lumen than non-thin-cap IVUS-derived TCFA. Thus, %plaque-volume, vessel remodelling index, confluent major NCCL area, and degree of NCCL circumference were the identifying factors for definite-TCFA by VH-IVUS. One of the clinical implications of the present study was to identify the VH-IVUS indices useful for diagnosing definite-TCFA.

Limitations

Because patients excluded from the study were those with high risk-ACS, we could not reach any conclusions about the general prevalence of definite-TCFA. Further, we could observe only limited vessel areas, as the VH-IVUS and OCT procedures have several limitations for imaging certain lesions, such as severely calcified tortuous lesions or other complex lesions. Thus, our study results do not represent an unbiased sampling of all coronary arteries, and the detection rate of TCFA in our study patients might be underestimated.

There were three cases of definite-TCFA with progression requiring PCI; it is unclear whether the detected definite-TCFA will cause acute coronary events and was a true vulnerable plaque. Although the frequency of the progression was too low to reach any statistical significance, definite-TCFA tended to progress more compared with non-TCFA. Our findings, therefore, should be confirmed with a larger study population and the subsequent course of the lesions observed as well.

In the present study, 61 plaques were identified as IVUS-derived TCFA by VH-IVUS examination. This identification was based on the criteria of a previous published report.[13] This high prevalence of high-risk plaque, however, was at variance with previously published *in vivo* and *in vitro* studies,[5,13] which might be because of inaccurate VH determination by *in vitro* testing. Further, we selected cut-off values of IVUS-derived TCFA criteria as %plaque-volume $>40\%$ and %necrotic-core $>10\%$ because pathologic TCFA is very unlikely to be present in segments with $<40\%$ occlusive lesion, and nearly 90% of ruptured plaque comprised $>10\%$ necrotic core in the plaque area.[3] We did consider that the necrotic core size of 10% was too low, because the average %necrotic-core of definite-TCFA was $20.0 \pm 6.8\%$ and that of non-TCFA was $15.3 \pm 8.6\%$. This data is in line with the previous pathologic findings in this subset of lesions and also in previous VH-IVUS studies.[2,3,14] Thus, TCFA might be over-diagnosed if based on the current definition of IVUS-derived TCFA. Our study population was too small, however, to establish new criteria for defining IVUS-derived TCFA.

Although we could perform the VH-IVUS and OCT procedures within 20 min and without complications, the combined use of VH-IVUS and OCT is laborious and costly. A new device with both IVUS and OCT functions to enable the simultaneous use of both modalities should be developed.

Conclusions

This is the first study to evaluate TCFA using a combination of two new imaging modalities, VH-IVUS and OCT. Neither modality alone is sufficient for detecting TCFA. The combined use of these complementary imaging modalities, VH-IVUS and OCT, however, should be considered a feasible approach for more precise detection of TCFA.

Conflict of interest: none declared.

Funding

Funding to pay the Open Access publication charges for this article will be provided by Dr Junya Shite.

References

1. Falk E, Shah PK, Fuster V. Coronary plaque disruption. *Circulation* 1995;**92**:657–671.
2. Kolodgie FD, Virmani R, Burke AP, Farb A, Weber DK, Kutys R, Finn AV, Gold HK. Pathologic assessment of the vulnerable human coronary plaque. *Heart* 2004;**90**:1385–1391.
3. Virmani R, Burke AP, Farb A, Kolodgie FD. Pathology of the vulnerable plaque. *J Am Coll Cardiol* 2006;**47**:C13–C18.
4. Arbustini E, Dal Bello B, Morbini P, Burke AP, Bocciarelli M, Specchia G, Virmani R. Plaque erosion is a major substrate for coronary thrombosis in acute myocardial infarction. *Heart* 1999;**82**:269–272.
5. Virmani R, Kolodgie FD, Burke AP, Farb A, Schwartz SM. Lessons from sudden coronary death a comprehensive morphological classification scheme for atherosclerotic lesions. *Arterioscler Thromb Vasc Biol* 2000;**20**:1262–1275.
6. Nair A, Margolis MP, Kuban BD, Vince DG. Automated coronary plaque characterization with intravascular ultrasound backscatter: *ex vivo* validation. *EuroIntervention* 2007;**3**:113–120.
7. Nasu K, Tsuchikane E, Katoh O, Vince DG, Virmani R, Surmely JF, Murata A, Takeda Y, Ito T, Ehara M, Matsubara T, Terashima M, Suzuki T. Accuracy of in vivo coronary plaque morphology assessment: a validation study of in vivo virtual histology compared with in vitro histopathology. *J Am Coll Cardiol* 2006;**47**:2405–2412.
8. Matsumoto D, Shite J, Shinke T, Otake H, Tanino Y, Ogasawara D, Sawada T, Paredes OL, Hirata KI, Yokoyama M. Neointimal coverage of sirolimus-eluting stents at 6-month follow-up: evaluated by optical coherence tomography. *Eur Heart J* 2007;**28**:961–967.
9. Jang IK, Bouma BE, Kang DH, Park SJ, Park SW, Seung KB, Choi KB, Shishkov M, Schlendorf K, Pomerantsev E, Houser SL, Aretz HT, Tearney GJ. Visualization of coronary atherosclerotic plaques in patients using optical coherence tomography: comparison with intravascular ultrasound. *J Am Coll Cardiol* 2002;**39**:604–609.
10. Yabushita H, Bouma BE, Houser SL, Aretz T, Jang IK, Schlendorf KH, Kauffman CR, Shishkov M, Kang DH, Halpen EF, Tearney GJ. Characterization of human atherosclerosis by optical coherence tomography. *Circulation* 2002;**106**:1640–1645.
11. Jang IK, Tearney GJ, MacNeill B, Takano M, Moselewski F, Iftima N, Shishkov M, Houser S, Aretz HT, Halpern EF, Bouma BE. In vivo characterization of coronary atherosclerotic plaque by use of optical coherence tomography. *Circulation* 2005;**111**:1551–1555.
12. Mintz GS, Nissen SE, Anderson WD, Bailey SR, Erbel R, Fitzgerald PJ, Pinto FJ, Rosenfield K, Siegel RJ, Tuzuc EM, Yock PG. American College of Cardiology Clinical Expert Consensus Document on Standards for Acquisition, Measurement and

Reporting of Intravascular Ultrasound Studies (IVUS). A report of the American College of Cardiology Task Force on Clinical Expert Consensus Documents. *J Am Coll Cardiol* 2001;**37**:1478–1492.
13. Rodriguez-Granillo GA, Garcia-Garcia HM, Mc Fadden EP, Valgimigli M, Aoki J, de Feyter P, Serruys PW. In Vivo intravascular ultrasound-derived thin-cap fibroatheroma detection using radiofrequency data analysis. *J Am Coll Cardiol* 2005;**46**:2038–2042.
14. Garcia-Garcia HM, Goedhart D, Schuurbiers JC, Kukreja N, Tanimoto S, Daemen J, Morel MA, Bressers M, van Es GA, Wentzel JJ, Gijsen F, van der Steen AF, Serruys PW. Virtual histology and remodeling index allow in vivo identification of allegedly high-risk coronary plaques in patients with acute coronary syndromes: a three vessel intravascular ultrasound rediofrequency data analysis. *EuroIntervention* 2006;**2**:338–344.
15. Burke AP, Farb A, Malcom GT, Liang YH, Smialek J, Virmani R. Coronary risk factors and plaque morphology in men with coronary disease who died suddenly. *N Eng J Med* 1997;**336**:1276–1282.
16. Burke AP, Kolodgie FD, Farb A, Weber D, Virmani R. Morphological predictors of arterial remodeling in coronary atherosclerosis. *Circulation* 2002;**105**:297–303.
17. Yamagishi M, Terashima M, Awano K, Kijima M, Nakatani S, Daikoku S, Ito K, Yasumura Y, Miyatake K. Morphology of vulnerable coronary plaque: Insights from follow-up of patients examined by intravascular ultrasound before an acute coronary syndrome. *J Am Coll Cardiol* 2000;**35**:106–111.
18. Ohtani T, Ueda Y, Mizote I, Oyabu J, Okada K, Hirayama A, Kodama K. Number of yellow plaques detected in a coronary artery is associated with future risk of acute coronary syndrome: detection of vulnerable patients by angioscopy. *J Am Coll Cardiol* 2006;**47**:2194–2200.
19. de Korte CL, Scharr JA, Mastik F, Serruys PW, van der Steen AF. Intravascular elastography: from bench to bedside. *J Interv Cardiol* 2003;**16**:253–259.
20. Madjid M, Willerson JT, Casscells SW. Intracoronary thermography for detection of high-risk vulnerable plaques. *J Am Coll Cardiol* 2006;**47**:C80–C85.
21. Manfrini O, Mont E, Leone O, Arbustini E, Eusebi V, Virmani R, Bugiardini R. Sources of error and interpretation of plaque morphology by optical coherence tomography. *Am J Cardiol* 2006;**98**:156–159.
22. Schoenhagen P, Ziada KM, Kapadia SR, Crowe TD, Nissen SE, Tuzcu EM. Extent and direction of arterial remodeling in stable versus unstable coronary syndromes: an intravascular ultrasound study. *Circulation* 2000;**101**:598–603.
23. Varnava AM, Mills PG, Davies MJ. Relationship between coronary artery remodeling and plaque vulnerability. *Circulation* 2002;**105**:939–943.